Optics Communications 298–299 (2013) 141–144

Contents lists available at SciVerse ScienceDirect

Optics Communications

journal homepage: www.elsevier.com/locate/optcom

Wide-spectrum optical hyperbolic metamaterial based on reverse hexagonal lyotropic liquid crystal

Xiaoping Li [a,b], Chengliang Yang [a], Dan Jia [a,b], Zhaoliang Cao [a], Quanquan Mu [a], Lifa Hu [a], Zenghui Peng [a], Yonggang Liu [a], Lishuang Yao [a], Xinghai Lu [a], Li Xuan [a,*]

[a] State Key Laboratory of Applied Optics, Changchun Institute of Optics, Fine Mechanics and Physics, Chinese Academy of Sciences, Changchun 130033, China
[b] University of Chinese Academy of Sciences, Beijing 100039, China

ARTICLE INFO

Article history:
Received 2 November 2012
Received in revised form
15 January 2013
Accepted 3 February 2013
Available online 28 February 2013

Keywords:
Metamaterial
Liquid crystal
Negative refraction
Dye molecules

ABSTRACT

Reverse hexagonal lyotropic liquid crystal template is proposed to achieve optical hyperbolic metamaterial composed of silver nanowire arrays. All angle negative refraction is obtained during the wide wavelength range from near-infrared to visible light. Hyperbolic metamaterial incorporated with gain dye molecules is calculated to show the possibility of eliminating energy losses and the transmittance can be enhanced in the selected wavelength range.

1. Introduction

There has been enormous interest in exploiting extraordinary properties of negative index metamaterial with negative permittivity and negative permeability simultaneously, which was originally proposed by Veselago [1]. Negative index metamaterial has been realized in the structure consisting of metallic wire arrays and split-ring resonators in the microwave regime [2,3] and metal–dielectric fishnet nanostructures in near-infrared wavelength range [4–6].

Compared with negative index metamaterial, hyperbolic metamaterial which has opposite signs of permittivity tensors could be used to realize negative refraction easily in optical frequency range. There are many advantages of hyperbolic metamaterial, such as needless negative permeability which leads to simplified design and broad band all-angle negative refraction [7]. Negative refraction from near-infrared to visible spectrum in hyperbolic metamaterial composed of silver nanowires embedding anodization aluminum oxide (AAO) template has been demonstrated experimentally [8–10]. However, negative refraction in silver–AAO metamaterial cannot be achieved in short wavelength due to the limitation of dielectric permittivity for aluminum oxide. So, one alternative approach is to select nano-size matrix template with small dielectric permittivity to fabricate hyperbolic metamaterial. In addition, silver–AAO metamaterial suffers inevitable strong energy dissipation due to plasmon resonance in the interface between metallic nanowires and aluminum oxide template. Low loss characteristic of hyperbolic metamaterial in optical frequency is critical for enabling its numerous potential applications, such as hyperlens [11]. Up to now, the way through improving the material geometric designs to reduce energy loss appears to reach its limitations. The most promising approach is to incorporate gain media into metamaterial [12]. Recently, the loss compensation in fishnet metamaterial with organic dyes incorporated in metal–dielectric spacer layers has been demonstrated experimentally [13]. The effect of loss compensation arises from the local field enhancement of the structures with gain media. For silver–AAO metamaterial, because AAO is a solid template, it is impossible to add gain medium into the structures.

Liquid crystals acting as tunable material have been extensively used in metamaterial structures [14–16] and are also proposed to achieve loss compensation by incorporating gain dye molecules [17,18]. In this paper, we use an alternative approach in which reverse hexagonal lyotropic liquid crystal (RHLLC) is used to reconfigure hyperbolic metamaterial. Proposed hyperbolic metamaterial is made up of metallic nanowires embedded in RHLLC.

2. Negative refraction

The RHLLC template is schematically shown in Fig. 1, and the structure parameters are in tens of nanometers scale [19,20]. By the self-assembly process hexagonal structure is formed utilizing water and amphiphilic molecule dissolved into solvent in an appropriate

* Corresponding author.
E-mail address: xuanli@ciomp.ac.cn (L. Xuan).

0030-4018/$ - see front matter © 2013 Published by Elsevier B.V.
http://dx.doi.org/10.1016/j.optcom.2013.02.017

concentration ratio at given a temperature. Silver nanowire arrays with uniform wire diameters, high aspect ratio and high wire density in RHLLC have been fabricated experimentally by electrochemical deposition [21]. The RHLLC are composed of ternary mixture p-xylene/AOT/water in restricted concentration ratio.

In the long wavelength limit (λ»a), the structure of RHLLC and embedded silver nanowires is equivalent to an effective medium which can be described by macroscopic anisotropic dielectric tensor $\varepsilon_{||}$ and $\varepsilon_{\perp}$ (parallel and perpendicular to metallic nanowires respectively). The effective medium theory is adopted for anisotropic nanowires system as follows [22]:

$$\begin{aligned} \varepsilon_{||} &= \varepsilon_z = f\varepsilon_m + (1-f)\varepsilon_{LLC} \\ \varepsilon_{\perp} &= \varepsilon_x = \varepsilon_{LLC}\left[\frac{(1+f)\varepsilon_m + (1-f)\varepsilon_{LLC}}{(1-f)\varepsilon_m + (1+f)\varepsilon_{LLC}}\right] \end{aligned} \quad (1)$$

where $f = 2\pi r^2/\sqrt{3}a^2$ is the volume filling ratio of silver nanowires in the composite structure. ε_m and ε_{LLC} are the permittivities of silver and RHLLC respectively. Permittivity of silver obeys the drude model which can be written as $\varepsilon_m = \varepsilon_\infty - \omega_p^2/(\omega^2 + i\omega\gamma)$, where the angular frequency $\omega = 2\pi c/\lambda$, the high frequency permittivity $\varepsilon_\infty = 6$, the plasma frequency $\omega_p = 1.5 \times 10^{16} rad/s$ and the damping frequency $\gamma = 7.73 \times 10^{13}$ rad/s are taken from the literature [23]. The refractive index of RHLLC is 1.46 determined by experimental measurement in which component fractions with 1.4 M AOT in p-xylene and molar ratio [H_2O]/[AOT] = 10 are adopted.

Effective anisotropic permittivities calculated are shown in Fig. 2. Typical sizes of a = 40 nm and r = 10 nm derived from experimental values in Ref. [21] (corresponding filling ratio f = 0.227) are used to make a comparison with AAO whose permittivity is assumed to be 2.7889 [24]. Hyperbolic dispersion curves of metamaterial produce all-angle negative refraction for TM polarized light (magnetic field normal to the plane of incidence, i.e. x–z plane as shown in Fig. 1(b)). Although the condition of hyperbolic dispersion relation with $\mathrm{Re}(\varepsilon_{||}) < 0$ and $\mathrm{Re}(\varepsilon_{\perp}) > 0$ is satisfied in the whole visible wavelength range, the resonant peaks of $\varepsilon_{\perp}$ would result in extremely large energy losses which severely destroy the validity of negative refraction. Thus, we have to choose a wavelength range far away from the resonant peak to ensure energy transmission for negative refraction. In this paper, the criterion $\mathrm{Im}(\varepsilon_{\perp}) < 0.1$ is chosen to determine the shortest wavelength for available negative refraction. As shown in Fig. 2(c) and (d), in silver–RHLLC metamaterial, the shortest wavelength satisfying the criterion is approximately 470 nm, almost 40 nm is enhanced compared to the silver–AAO metamaterial. We can see that $\varepsilon_{||}$ is almost the same in two kinds of metamaterial, shown in Fig. 2(a) and (b). The resonant peaks appear when $\mathrm{Re}(\varepsilon_{\perp}) = 0$. Due to the smaller permittivity of RHLLC, resonant peak shifts to shorter wavelength which is the reason why silver–RHLLC can realize negative refraction in a shorter wavelength range. Thus, negative refraction for silver–RHLLC metamaterial covers the spectrum from approximately 470 nm up to near-infrared wavelength range.

The working spectrum range for hyperbolic metamaterial mainly depends on two parameters, nanoholes distance and nanowire radius. In actual experimental operations, nanoholes distance is approximately unchangeable, but the nanowire radius can be adjusted by changing the component concentration. Here, we focus on the effect of radius for the working spectrum of hyperbolic metamaterial. Nanoholes distance is fixed (40 nm); we choose different radii r = 6 nm, 8 nm, 10 nm, 12 nm and 14 nm, which correspond to volume filling ratios f = 0.082, 0.145, 0.227, 0.326 and 0.444 respectively. As shown in Fig. 3, the working wavelength for $\mathrm{Re}(\varepsilon_{||}) < 0$ is blue shifted as the radius increases; on the contrary the wavelength satisfying $\mathrm{Im}(\varepsilon_{\perp}) < 0.1$ is red shifted. The working spectrum range must satisfy both the criterions $\mathrm{Re}(\varepsilon_{||}) < 0$ and $\mathrm{Im}(\varepsilon_{\perp}) < 0.1$. According to the figure, optimized radius is 10 nm and the wavelengths satisfying the two criterions are almost the same. The corresponding working wavelength is approximately started from 470 nm. The optimization for working wavelength range of silver–RHLLC hyperbolic metamaterial is achieved through calculations.

3. Loss compensation

Because of the existence of silver nanowires the proposed metamaterial suffers strong energy losses. Here, we also investigate the loss compensation in the silver–RHLLC metamaterial.

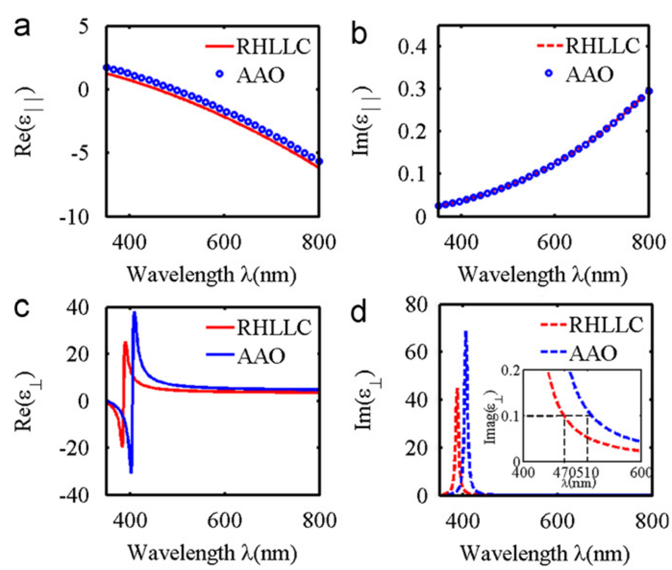

Fig. 2. Effective anisotropic permittivities for silver–RHLLC metamaterial and silver–AAO metamaterial. (a) and (b) Real part and imaginary part of $\varepsilon_{||}$. (c) and (d) Real part and imaginary part of $\varepsilon_{\perp}$. The inset in (d) is the magnified part in the range $\lambda = 400-600$ nm.

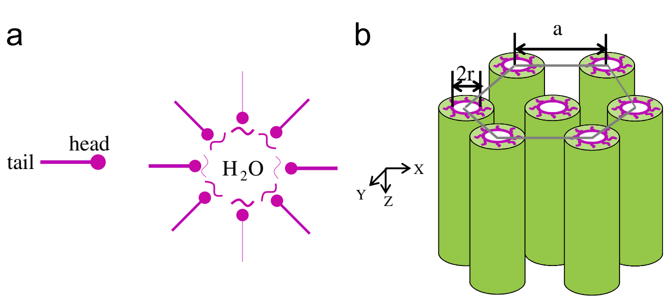

Fig. 1. (a) Schematic diagram of amphiphilic molecule hexagonal structure. (b) The RHLLC template structure. a is the distance of adjacent nanoholes and r is the radius of nanoholes.

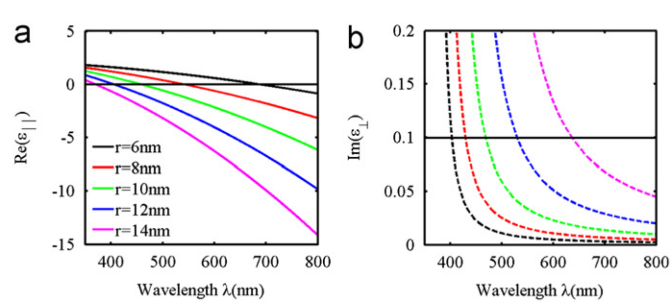

Fig. 3. Real parts of $\varepsilon_{||}$ and imaginary parts of $\varepsilon_{\perp}$ for different radii of silver nanowires.

Due to the RHLLC which is a liquid template, the gain media can be incorporated conveniently into the metamaterial structures, such as fluorescent dyes. Here, the dielectric susceptibility of gain dye molecules described as the four-level system model is characterized by the form $\chi = \chi' + i\chi''$, where the real part χ' and imaginary part χ'' are written as follows [25]:

$$\chi' = \chi_{max} \frac{1}{1+I_0/I_s} \frac{2(\nu-\nu_0)/\Delta\nu}{1+4(\nu-\nu_0)^2/\Delta\nu^2}$$
$$\chi'' = \chi_{max} \frac{1}{1+I_0/I_s} \frac{1}{1+4(\nu-\nu_0)^2/\Delta\nu^2} \quad (2)$$

where I_s is the saturation intensity and I_0 is the pump intensity. χ_{max} is the maximum imaginary value at low intensities ($I_0 \ll I_s$) and ν is the incident frequency. The parameters are chosen as follows: the center frequency $\nu_0 = 5.639 \times 10^{14}$Hz and the transition linewidth $\Delta\nu = 5.639 \times 10^{12}$Hz. The structure parameters are the same as mentioned above in part 2. From formula (2), when ν_0 and $\Delta\nu$ are fixed, the dielectric susceptibility of gain dye molecules depends on χ_{max} and I_0/I_s.

When gain dye molecules are incorporated into RHLLC, the permittivity of the host RHLLC template $\varepsilon'_{LLC} = \varepsilon_{LLC} + \chi$ is modified slightly and is substituted into effective medium calculations based on formula (1). In calculations, $\chi_{max} = -0.03$ is assumed and the ε'_{LLC} is only associated with I_0/I_s. As indicated in Fig. 4 the values of $\mathrm{Im}(\varepsilon_{||})$ and $\mathrm{Im}(\varepsilon_{\perp})$ for gain incorporation decrease remarkably compared to without gain. For small I_0/I_s, smaller imaginary part value can be obtained. With the value I_0/I_s increasing, the imaginary part gets closer to the value of no gain. In addition, the shapes for $\mathrm{Re}(\varepsilon_{||})$ and $\mathrm{Re}(\varepsilon_{\perp})$ (not shown) only have slight change between metamaterial with gain and without gain. Highly decreased imaginary values of $\varepsilon_{||}$ and $\varepsilon_{\perp}$ lead to the reduction of energy losses in metamaterial.

Energy compensation in metamaterial originates from optical amplification in the RHLLC matrix and loss compensation for plasmonic resonance of nanowires at gain pumping wavelengths. Using the finite element method, the transmittance is simulated for without and with gain metamaterial as shown in Fig. 5. $\chi_{max} = -0.03$ is assumed and we mainly consider the effect of incident intensity for transmittance. From Fig. 5, we can see that the transmittance around wavelength 532 nm for gain metamaterial increases compared with no gain, which means optical energy compensation in the constituent metamaterial. The simulation illustrates that the gain incorporation can improve the transmittance remarkably. In addition, simulations also show that larger transmittance could be obtained when incident intensity is far away from the saturation intensity.

χ_{max} is proportional to the real and imaginary part of susceptibility of the gain dye molecule. From formula (2), different gain materials with different χ_{max} values would impact the transmittance of metamaterial. Incident intensity ratio $I_0/I_s = 0.1$ is fixed. Fig. 6 shows the simulated transmittance for different gain materials. We can see that transmittance increases remarkably as χ_{max} changes from -0.03 to -0.09. Central peak transmittances are 0.88, 1.00 and 1.22 respectively for $\chi_{max} = -0.03, -0.06, -0.09$. Transmittance equal to 1 for $\chi_{max} = -0.06$ means that energy dissipation is completely compensated by gain materials. When $\chi_{max} = -0.09$ the transmittance is more than 1 which means optical amplifications are due to the gain materials. Larger transmittance could also be obtained by taking other gain materials with larger $\chi_{\max}$ for much stronger energy compensation. Actually the gain dye molecule is only functional at the specific working spectrum, so loss compensation for other wavelength can be realized by choosing the appropriate gain dyes. The bandwidth of transmittance enhancement is highly related to the linewidth $\Delta\nu$.

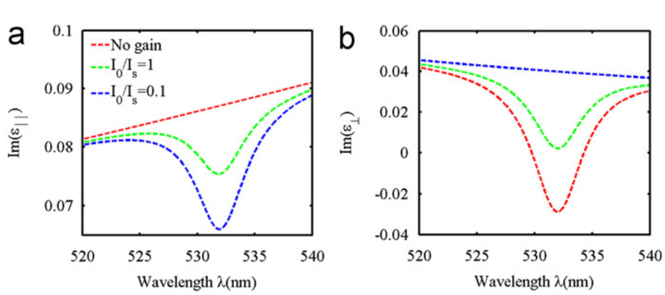

Fig. 4. The imaginary parts of $\varepsilon_{||}$ and $\varepsilon_{\perp}$ for the sample without and with gain ($\chi_{\max} = -0.03$) around center frequency $\nu_0 = 5.639 \times 10^{14}$ Hz (wavelength $\lambda = 532$ nm).

4. Conclusions

In conclusion, we propose an alternative approach for optical hyperbolic metamaterial consisting of silver nanowire arrays embedded in RHLLC template. Negative refraction at visible spectrum up to approximately 470 nm can be achieved through silver–RHLLC metamaterial. Incorporating gain media into RHLLC metamaterial is a very convenient and effective route for

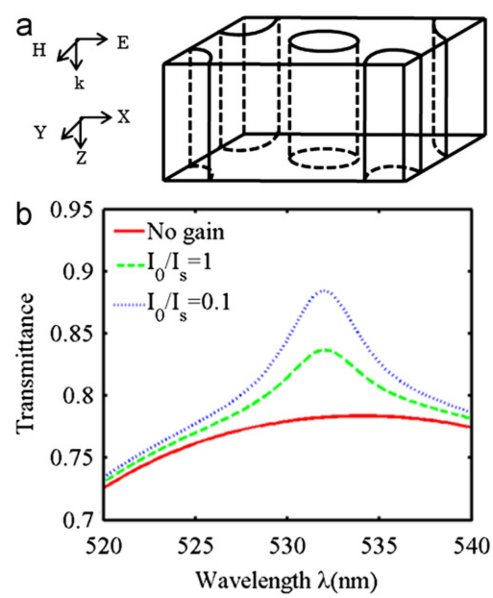

Fig. 5. (a) Basic structural unit in simulation. The slice thickness is 500 nm. Periodic boundary condition is used. (b) The transmittance for without and with gain ($\chi_{max} = -0.03$). Structure parameters are a=40 nm, r=10 nm.

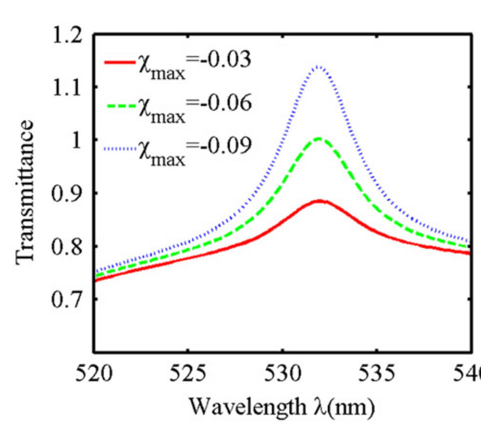

Fig. 6. The transmittance for different χ_{max} values.

compensating energy dissipation. Transmittance of designed silver–RHLLC metamaterial with gain can be improved at selected wavelength. The fabrication of the proposed silver–RHLLC metamaterial can be accomplished easily with an inexpensive self-assemble process and electrochemical deposition method [21]. Finally, the flexible RHLLC template can also be used for other structure fabrications with potential applications such as hyperlens and cloaking [26].

Acknowledgment

This work is supported by the National Science Foundation of China (11174274, 61205021, 11204299 and 11174279) and the Foundation of State Key Laboratory of Applied Optics.

References

[1] V.G. Veselago, Physics-Uspekhi 10 (1968) 509.
[2] R.A. Shelby, D.R. Smith, S. Schultz, Science 292 (2001) 77.
[3] C.G. Parazzoli, R.B. Greegor, K. Li, B.E.C. Koltenbah, M. Tanielian, Physical Review Letters 90 (2003) 107401.
[4] S. Zhang, W. Fan, N.C. Panoiu, K.J. Malloy, R.M. Osgood, S.R.J. Brueck, Physical Review Letters 95 (2005) 137404.
[5] G. Dolling, C. Enkrich, M. Wegener, C.M. Soukoulis, S. Linden, Science 312 (2006) 892.
[6] J. Valentine, S. Zhang, T. Zentgraf, E. Ulin-Avila, D.A. Genov, G. Bartal, X. Zhang, Nature 455 (2008) 376.
[7] R. Wangberg, J. Elser, E.E. Narimanov, V.A. Podolskiy, Journal of the Optical Society of America B–Optical Physics 23 (2006) 498.
[8] J. Yao, Z. Liu, Y. Liu, Y. Wang, C. Sun, G. Bartal, A.M. Stacy, X. Zhang, Science 321 (2008) 930.
[9] M.A. Noginov, Y.A. Barnakov, G. Zhu, T. Tumkur, H. Li, E.E. Narimanov, Applied Physics Letters 94 (2009) 151105.
[10] J. Kanungo, J. Schilling, Applied Physics Letters 97 (2010) 021903.
[11] Z. Jacob, L.V. Alekseyev, E. Narimanov, Optics Express 14 (2006) 8247.
[12] S.A. Ramakrishna, J.B. Pendry, Physical Review B 67 (2003) 201101.
[13] S. Xiao, V.P. Drachev, A.V. Kildishev, X. Ni, U.K. Chettiar, H.K. Yuan, V.M. Shalaev, Nature 466 (2010) 735.
[14] I.C. Khoo, D.H. Werner, X. Liang, A. Diaz, B. Weiner, Optics Letters 31 (2006) 2592.
[15] D.H. Werner, D.H. Kwon, I.C. Khoo, Optics Express 15 (2007) 3342.
[16] X. Wang, D.H. Kwon, D.H. Werner, I.C. Khoo, A.V. Kildishev, V.M. Shalaev, Applied Physics Letters 91 (2007) 143122.
[17] I.C. Khoo, A. Diaz, J. Liou, M.V. Stinger, J.B. Huang, Y. Ma, IEEE Journal of Selected Topics in Quantum Electronics 16 (2010) 410.
[18] O.D. Lavrentovich, Proceedings of the National Academy of Sciences 108 (2011) 5143.
[19] P. Ekwall, L. Mandell, K. Fontell, Molecular Crystals and Liquid Crystals 8 (1969) 157.
[20] P. Alexandridis, U. Olsson, B. Lindman, Langmuir 14 (1998) 2627.
[21] L. Huang, H. Wang, Z. Wang, A. Mitra, K.N. Bozhilov, Y.S. Yan, Advanced Materials 14 (2002) 61.
[22] Y. Liu, G. Bartal, X. Zhang, Optics Express 16 (2008) 15439.
[23] P.B. Johnson, R.W. Christy, Physical Review B 6 (1972) 4370.
[24] H. Masuda, M. Ohya, H. Asoh, M. Nakao, M. Nohtomi, T. Tamamura, Japanese Journal of Applied Physics 38 (1999) L1403.
[25] A. Yariv, Photonics: Optical Electronics in Modern Communications, Oxford University Press, New York, 2007.
[26] J.B. Pendry, D. Schurig, D.R. Smith, Science 312 (2006) 1780.